

Table of contents

1. Synthesis of substituted aromatic derivatives using melted $\text{FeCl}_3 \cdot 6\text{H}_2\text{O}$	2
1.1 General procedures	2
Bromination	2
Nitration.....	2
Thiocyanation	2
1.2 Spectroscopic characterisation of the products	2
1.2.1 Characterisation of brominated products.....	3
1.3.2 Characterisation of the nitrated products.....	4
1.3.3 Characterisation of the thiocyanated products	6
1.3 Condition optimisation for the bromination of aromatic derivatives without any co-oxidant	7
1.4 PCA analysis of the conditions for bromination reaction	8
2. Spectroscopic analyses of $\text{FeCl}_3 \cdot 6\text{H}_2\text{O}$	9
2.1 Characterisation of $\text{FeCl}_3 \cdot 6\text{H}_2\text{O}$	9
2.1.1 Raman studies	9
2.1.2 Direct injection mass spectrometry studies.....	10
2.2 Characterisation of $\text{FeCl}_3 \cdot 6\text{H}_2\text{O}$ in presence of NaBr	10
2.3 Characterisation of $\text{FeCl}_3 \cdot 6\text{H}_2\text{O}$ in presence of KNO_3	11
2.4 Characterisation of $\text{FeCl}_3 \cdot 6\text{H}_2\text{O}$ in presence of KSCN	11
3. Computational calculations	12
3.1 Methods	12
3.2 DFT calculations of the ion pair complexes	13
3.2.1 Procedure	13
3.2.2 Choice of the system studied	13
3.2.3 Results - Optimised geometry and Gibbs free energy.....	17
3.2.4 Results – Partial atomic charges of the optimised conformers	19
3.3 DFT calculations of the ion pair complexes in presence of anisole	23
3.3.1 Procedure	23
3.3.2 Results - Optimised geometry and Gibbs free energy.....	24
3.3.3 Results – Partial atomic charges of the optimised conformers	25
References	29

1. Synthesis of substituted aromatic derivatives using melted $\text{FeCl}_3 \cdot 6\text{H}_2\text{O}$

1.1 General procedures

Reagents and solvents were purchased from Sigma-Aldrich, and were used without further purification.

Bromination

Methoxy arene (0.5 mmol), sodium bromine (51.5 mg, amount corresponding to 0.50 mmol) and $\text{FeCl}_3 \cdot 6\text{H}_2\text{O}$ (270.3 mg, amount corresponding to 1 mmol) were introduced in a sealed tube (ace glass tube, 10.2 cm x 25.4 mm) with a magnetic stirring bar and heated to 80°C in oil bath for 24 h until completion of the reaction. The reaction mixture was then diluted with an ethyl acetate/water mixture (10 /10 mL). The product is extracted three times with ethyl acetate (3 x 5 mL), washed with water (5 mL) and dried over MgSO_4 . The organic phase was concentrated under reduced pressure and diluted in dichloromethane before GC-MS analysis. The analyses and yields were also confirmed by ^1H and ^{13}C NMR analyses.

Nitration

Methoxy arene (0.5 mmol), potassium nitrate (50.6 mg, amount corresponding to 0.50 mmol) and $\text{FeCl}_3 \cdot 6\text{H}_2\text{O}$ (135.2 mg, amount corresponding to 0.5 mmol) were introduced in a sealed tube (ace glass tube, 10.2 cm x 25.4 mm) with a magnetic stirring bar and heated to 60°C in oil bath for 6 h until completion of the reaction. The reaction mixture was then diluted with an ethyl acetate/water mixture (10 /10 mL). The product is extracted three times with ethyl acetate (3 x 5 mL), washed with water (5 mL) and dried over MgSO_4 . The organic phase was concentrated under reduced pressure and diluted in dichloromethane before GC-MS analysis. The analyses and yields were also confirmed by ^1H and ^{13}C NMR analyses.

Thiocyanation

Methoxy arene (0.5 mmol), potassium thiocyanate (48.6 mg, amount corresponding to 0.50 mmol) and $\text{FeCl}_3 \cdot 6\text{H}_2\text{O}$ (270.3 mg, amount corresponding to 1 mmol) were introduced in a sealed tube (ace glass tube, 10.2 cm x 25.4 mm) with a magnetic stirring bar and heated to 80°C in oil bath for 6 h until completion of the reaction. The reaction mixture was then diluted with an ethyl acetate/water mixture (10 /10 mL). The product is extracted three times with ethyl acetate (3 x 5 mL), washed with water (5 mL) and dried over MgSO_4 . The organic phase was concentrated under reduced pressure and diluted in dichloromethane before GC-MS analysis. The analyses and yields were also confirmed by ^1H and ^{13}C NMR analyses.

1.2 Spectroscopic characterisation of the products

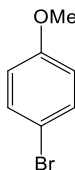
Gas chromatography and mass spectrometry (GC-MS) analyses were performed using a TRACETM 1300 apparatus equipped with an ISQTM QD mass spectrometer detector (Thermo Fisher Scientific) coupled with an FID detector (Thermo Fisher scientific). Hydrogen was the carrier gas at a flow rate of 0.8 mL/min, and the program used was set as following: 80 °C for 1 min then heating to 260 °C with a rate of 45 °C/min followed by a linear gradient at 260 °C for 1 min.

NMR spectra were recorded on a Bruker Avance 400 spectrometer (Bruker), BBFO Probe, with acetone- d_6 as solvent (2.09 ppm for ^1H and 30.60 and 205.87 ppm for ^{13}C).

IR analyses were conducted using a Perkin-Elmer Spectrum 100 ATR-FT-IR spectrometer.

1.2.1 Characterisation of brominated products

4-bromoanisole (1)

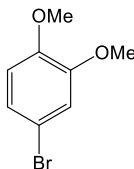


Yield: 78%, GC conversion: 100%

^1H NMR (400 MHz, $(\text{CD}_3)_2\text{CO}$): $\delta/\text{ppm} = 7.45\text{-}7.42$ (d, $J = 9.05$ Hz, 2H), $6.92\text{-}6.90$ (d, $J = 9.02$ Hz, 2H), 3.81 (s, 3H). ^{13}C NMR (100.6 MHz, $(\text{CD}_3)_2\text{CO}$): $\delta/\text{ppm} = 159.11, 132.15, 115.99, 112.08, 54.93$.

^1H and ^{13}C NMR spectra are in agreement with those previously reported.¹

4-bromo-1,2-dimethoxybenzene (2)

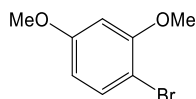


Yield: 51%, GC conversion: 100%.

^1H NMR (400 MHz, $(\text{CD}_3)_2\text{CO}$): $\delta/\text{ppm} = 7.08$ (d, $J = 2$ Hz, 1H), $7.06\text{-}7.04$ (m, 1H), $6.91\text{-}6.89$ (d, $J = 8.46$ Hz, 1H), 3.84 (s, 3H), 3.81 (s, 3H). ^{13}C NMR (100.6 MHz, $(\text{CD}_3)_2\text{CO}$): $\delta/\text{ppm} = 150.47, 149.02, 123.18, 115.05, 113.35, 112.07, 55.47, 55.36$.

^1H and ^{13}C NMR spectra are in agreement with those previously reported.²

1-bromo-2,4-dimethoxybenzene (3)

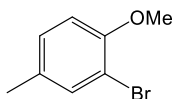


Yield: 51%, GC conversion: 97%

^1H NMR (400 MHz, $(\text{CD}_3)_2\text{CO}$): $\delta/\text{ppm} = 7.28\text{-}7.26$ (d, $J = 8.71$ Hz, 1H), $6.51\text{-}6.50$ (d, $J = 2.72$ Hz, 1H), $6.36\text{-}6.33$ (dd, $J = 2.74, J = 8.72$, 1H), 3.73 (s, 3H), 3.67 (s, 3H). ^{13}C NMR (100.6 MHz, $(\text{CD}_3)_2\text{CO}$): $\delta/\text{ppm} = 160.68, 156.72, 132.98, 106.40, 101.63, 99.86, 55.60, 55.04$.

^1H and ^{13}C NMR spectra are in agreement with those previously reported.¹

2-bromo-1-methoxy-4-methylbenzene (4)

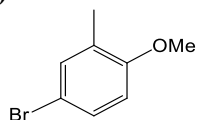


Yield: 64%, conversion GC: 86%

^1H NMR (400 MHz, $(\text{CD}_3)_2\text{CO}$): $\delta/\text{ppm} = 7.33\text{-}7.32$ (d, $J = 1.88$ Hz, 1H), $7.09\text{-}7.07$ (dd, $J = 1.71$ Hz, $J = 8.44$ Hz, 1H), $6.91\text{-}6.89$ (d, $J = 8.36$, 1H), 3.79 (s, 3H), 2.21 (s, 3H). ^{13}C NMR (100.6 MHz, $(\text{CD}_3)_2\text{CO}$): $\delta/\text{ppm} = 153.93, 133.40, 131.32, 129.13, 112.23, 110.77, 55.65, 19.19$.

^1H and ^{13}C NMR spectra are in agreement with those previously reported.¹

4-bromo-1-methoxy-2-methylbenzene (5)



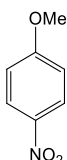
Yield: 74%, GC conversion: 100%

^1H NMR (400 MHz, $(\text{CD}_3)_2\text{CO}$): $\delta/\text{ppm} = 7.31\text{-}7.28$ (d, $J = 2.51$ Hz, 1H), 7.28 (s, 1H), 6.87-6.85 (d, $J = 8.26$, 1H), 3.83 (s, 3H), 2.17 (s, 3H). ^{13}C NMR (100.6 MHz, $(\text{CD}_3)_2\text{CO}$): $\delta/\text{ppm} = 157.11, 132.77, 129.42, 128.85, 111.92, 111.73, 55.03, 15.18$.

^1H and ^{13}C NMR spectra are in agreement with those previously reported.³

1.3.2 Characterisation of the nitrated products

1-methoxy-4-nitrobenzene (6a)

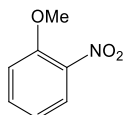


Yield: 25%, GC conversion: 40%

^1H NMR (400 MHz, $(\text{CD}_3)_2\text{CO}$): $\delta = 8.09\text{-}8.07$ (d, $J = 9.25$, 2H), 7.01-6.99 (d, $J = 9.21$ Hz, 2H), 3.82 (s, 3H). ^{13}C NMR (100.6 MHz, $(\text{CD}_3)_2\text{CO}$): $\delta = 164.91, 126.38, 125.68, 114.32, 55.73$.

^1H and ^{13}C NMR spectra are in agreement with those previously reported.²

1-methoxy-2-nitrobenzene (6b)

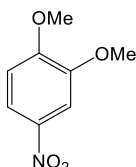


Yield: 15%, GC conversion: 40%

^1H NMR (400 MHz, $(\text{CD}_3)_2\text{CO}$): $\delta = 7.69\text{-}7.67$ (dd, $J = 1.53, J = 8.03$, 1H), 7.53-7.48 (m, 1H), 7.45-7.43 (d, $J = 8.86$, 1H), 7.21-7.19 (d, $J = 8.40$, 1H), 3.83 (s, 3H). ^{13}C NMR (100.6 MHz, $(\text{CD}_3)_2\text{CO}$): $\delta = 152.42, 134.04, 130.99, 124.83, 120.31, 113.92, 55.39$.

^1H and ^{13}C NMR spectra are in agreement with those previously reported.²

1,2-dimethoxy-4-nitrobenzene (7)

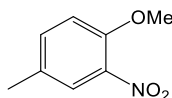


Yield: 92%, GC conversion: 100%

^1H NMR (400 MHz, $(\text{CD}_3)_2\text{CO}$): $\delta = 7.90\text{-}7.87$ (dd, $J = 2.67$ Hz, $J = 8.93$ Hz, 1H), 7.74 (d, $J = 2.66$ Hz, 1H), 7.15-7.12 (d, $J = 8.94$ Hz, 1H), 3.97 (s, 3H), 3.96 (s, 3H). ^{13}C NMR (100.6 MHz, $(\text{CD}_3)_2\text{CO}$): $\delta = 155.04, 149.23, 141.28, 117.28, 110.41, 106.28, 55.80, 55.60$.

^1H and ^{13}C NMR spectra are in agreement with those previously reported.⁴

1-methoxy-4-methyl-2-nitrobenzene (8a)

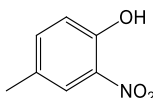


Yield: 36%, GC conversion: 85%

^1H NMR (400 MHz, $(\text{CD}_3)_2\text{CO}$): δ = 8.18 (s, 1H), 7.46-7.43 (dd, J = 1.81 Hz, J = 8.53 Hz, 1H), 7.22-7.19 (d, J = 8.55 Hz, 1H), 3.94 (s, 3H), 2.35 (s, 3H). ^{13}C NMR (100.6 MHz, $(\text{CD}_3)_2\text{CO}$): δ = 150.41, 138.51, 134.47, 129.72, 124.90, 113.83, 56.07, 19.13.

^1H and ^{13}C NMR spectra are in agreement with those previously reported.^{4,5}

4-methyl-2-nitrophenol (8b)

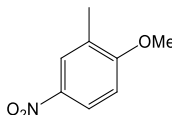


Yield: 36%, GC conversion: 85%

^1H NMR (400 MHz, $(\text{CD}_3)_2\text{CO}$): δ = 7.90-7.89 (d, J = 1.27 Hz, 1H), 7.53-7.50 (dd, J = 2.03 Hz, J = 8.52 Hz, 1H), 7.08-7.06 (d, J = 5.91 Hz, 1H), 3.75 (s, 1H), 2.24 (s, 3H). ^{13}C NMR (100.6 MHz, $(\text{CD}_3)_2\text{CO}$): δ = 152.58, 130.22, 129.29, 124.23, 119.58, 19.04.

^1H and ^{13}C NMR spectra are in agreement with those previously reported.⁶

1-methoxy-2-methyl-4-nitrobenzene (9a)

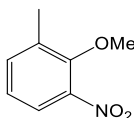


Yield: 65%, GC conversion: 100%

^1H NMR (400 MHz, $(\text{CD}_3)_2\text{CO}$): δ = 8.12-8.09 (dd, J = 2.71 Hz, J = 8.96 Hz, 1H), 8.04-8.03 (d, J = 2.29 Hz, 1H), 7.13-7.11 (d, J = 8.98 Hz, 1H), 4.00 (s, 3H), 2.27 (s, 3H). ^{13}C NMR (100.6 MHz, $(\text{CD}_3)_2\text{CO}$): δ = 163.00, 135.52, 127.62, 125.41, 123.48, 109.91, 55.83, 15.36.

^1H spectrum is in agreement with those previously reported.⁷

2-methoxy-1-methyl-3-nitrobenzene (9b)

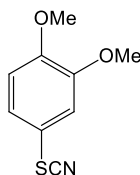


Yield: 17%, GC conversion: 100%

^1H NMR (400 MHz, $(\text{CD}_3)_2\text{CO}$): δ = 7.67-7.65 (d, J = 7.78 Hz, 1H), 7.55-7.53 (d, J = 8.22 Hz, 1H), 7.22 (t, J = 7.85 Hz, 1H), 3.90 (s, 3H), 2.38 (s, 3H). ^{13}C NMR (100.6 MHz, $(\text{CD}_3)_2\text{CO}$): δ = 151.10, 140.94, 135.04, 134.43, 124.04, 122.35, 61.37, 15.16.

1.3.3 Characterisation of the thiocyanated products

1,2-dimethoxy-4-thiocyanatobenzene (10)

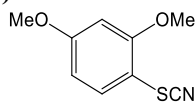


Yield: 59%, GC conversion: 67%

^1H NMR (400 MHz, $(\text{CD}_3)_2\text{CO}$): δ = 7.22 (m, 2 H), 7.08-7.06 (d, J = 9.02 Hz, 1 H), 3.89 (s, 3H), 3.87 (s, 3H). ^{13}C NMR (100.6 MHz, $(\text{CD}_3)_2\text{CO}$): δ = 151.43, 150.50, 125.17, 114.97, 113.81, 112.85, 55.59, 55.42.

IR: 2831, 2154 (SCN), 1583, 1501, 1251, 1230, 1176, 1137, 1018, 799, 764 cm^{-1} .

2,4-dimethoxy-1-thiocyanatobenzene (11)

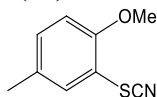


Yield: 84%, GC conversion: 100%

^1H NMR (400 MHz, $(\text{CD}_3)_2\text{CO}$): δ = 7.55-7.52 (d, J = 8.65 Hz, 1H), 6.77 -6.76 (d, J = 2.53 Hz, 1H), 6.72-6.70 (dd, J = 2.53 Hz, J = 8.64 Hz, 1H), 4.00 (s, 3H), 3.90 (s, 3H). ^{13}C NMR (100.6 MHz, $(\text{CD}_3)_2\text{CO}$): δ = 163.50, 159.28, 134.72, 133.79, 106.94, 101.84, 99.54, 55.96, 55.27.

IR: 2835, 2156 (SCN), 1573, 1453, 1279, 1208, 1161, 1066, 1020, 915, 823, 633. cm^{-1} .

2-methoxy-4-methyl-2-thiocyanatobenzene (12)

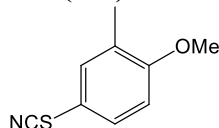


Yield: 55%, GC conversion: 78%

^1H NMR (400 MHz, $(\text{CD}_3)_2\text{CO}$): δ = 7.37 (d, J = 1.58 Hz, 1H), 7.26 (m, 1H), 7.07-7.05 (d, J = 8.53 Hz, 1H), 3.93 (s, 3H), 2.34 (s, 3H). ^{13}C NMR (100.6 MHz, $(\text{CD}_3)_2\text{CO}$): δ = 154.71, 133.62, 131.36, 129.88, 129.74, 113.56, 112.16, 55.99, 19.49.

IR: 2834, 2156 (SCN), 1579, 1494, 1247, 1065, 1020, 805, 739 cm^{-1} .

1-methoxy-2-methyl-4-thiocyanatobenzene (13a)



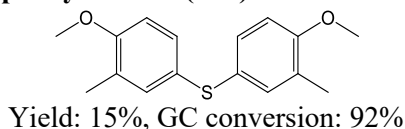
Yield: 56%, GC conversion: 92%

^1H NMR (400 MHz, $(\text{CD}_3)_2\text{CO}$): δ = 7.51-7.48 (ddd, J = 0.50 Hz, J = 2.53 Hz, J = 8.58 Hz, 1H), 7.45-7.44 (m, 1H), 7.08-7.07 (d, J = 8.60 Hz, 1H), 3.90 (s, 3H), 2.22 (s, 3H). ^{13}C NMR (100.6 MHz, $(\text{CD}_3)_2\text{CO}$): δ = 159.64, 133.91, 131.47, 129.08, 120.10, 113.18, 111.81, 55.26, 15.27.

IR: 2835, 2154 (SCN), 1590, 1490, 1247, 1135, 1026, 805, 751, 640 cm^{-1} .

Spectral data are in agreement with those previously reported.⁸

4,4'-Dimethoxy-3,3'-dimethyl diphenyl sulfide (13b)



^1H NMR (400 MHz, $(\text{CD}_3)_2\text{CO}$): δ = 7.18-7.17 (dd, J = 1.87 Hz, 1H), 7.15 (d, J = 0.65 Hz, 1H), 6.89 (t, J = 7.16 Hz, 1H), 3.82 (s, 3H), 2.14 (s, 3H). ^{13}C NMR (100.6 MHz, $(\text{CD}_3)_2\text{CO}$): δ = 157.37, 133.51, 130.33, 127.27, 126.76, 110.80, 109.93, 54.94, 15.36.

1.3 Condition optimisation for the bromination of aromatic derivatives without any oxidant

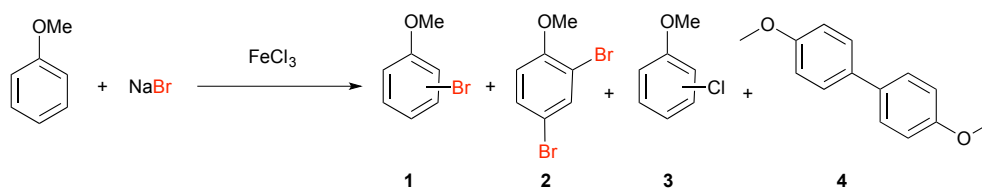


Table 1S. Bromination of anisole using anhydrous and hydrated FeCl_3 . NaBr , $\text{FeCl}_3 \cdot 6\text{H}_2\text{O}$ and anisole were put successively in a sealed tube under heating and magnetic stirring. Yields and conversions determined by GC-MS using dodecane as internal standard.

Entry	Fe source	Support	Solvent	Eq Fe	Eq NaBr	time (h)	T ($^{\circ}\text{C}$)	Conv (%)	Yields (%)			
									1	2	3	4
Using supports												
1	FeCl_3	SiO_2	-	1	1	24	80	31	21	-	-	6
2	FeCl_3	MK10	-	1	1	24	80	33	5	-	-	6
3	FeCl_3	MK10/molecular sieve	-	1	1	2	80	9.5	2	-	8	-
4	$\text{FeCl}_3 \cdot 6\text{H}_2\text{O}$	SiO_2	-	1	1	24	80	15	6	-	-	4
5	$\text{FeCl}_3 \cdot 6\text{H}_2\text{O}$	SiO_2	-	2	1	24	80	32	20	-	-	5
6	$\text{FeCl}_3 \cdot 6\text{H}_2\text{O}$	MK10	-	1	1	24	80	31	6	-	31	-
7	$\text{FeCl}_3 \cdot 6\text{H}_2\text{O}$	MK10/molecular sieve	-	1	1	2	80	2.5	2.5	-	-	-
Using solvents												
8	$\text{FeCl}_3 \cdot 6\text{H}_2\text{O}$	MK10	Cyclohexane	1	1	6	80	-	Traces	-	-	-
9	$\text{FeCl}_3 \cdot 6\text{H}_2\text{O}$	-	MeTHF	2	2	6	80	0	0	-	-	-
10	$\text{FeCl}_3 \cdot 6\text{H}_2\text{O}$	-	Diethylcarbonate	2	2	6	80	0	0	-	-	-
Solvent-free conditions												
11	$\text{FeCl}_3 \cdot 6\text{H}_2\text{O}$	-	-	2	1	6	80	100	75	Traces	-	-
12	$\text{FeCl}_3 \cdot 6\text{H}_2\text{O}$	-	-	2	1	24	80	93	85	Traces	-	Traces
13	$\text{FeCl}_3 \cdot 6\text{H}_2\text{O}$	-	-	2	1	6	60	16	15	-	-	-
14	$\text{FeCl}_3 \cdot 6\text{H}_2\text{O}$	-	-	2	1	6	100	100	39	35	-	-
15	$\text{FeCl}_3 \cdot 6\text{H}_2\text{O}$	-	-	2	4	6	80	100	44	26	-	-

1.4 PCA analysis of the conditions for bromination reaction

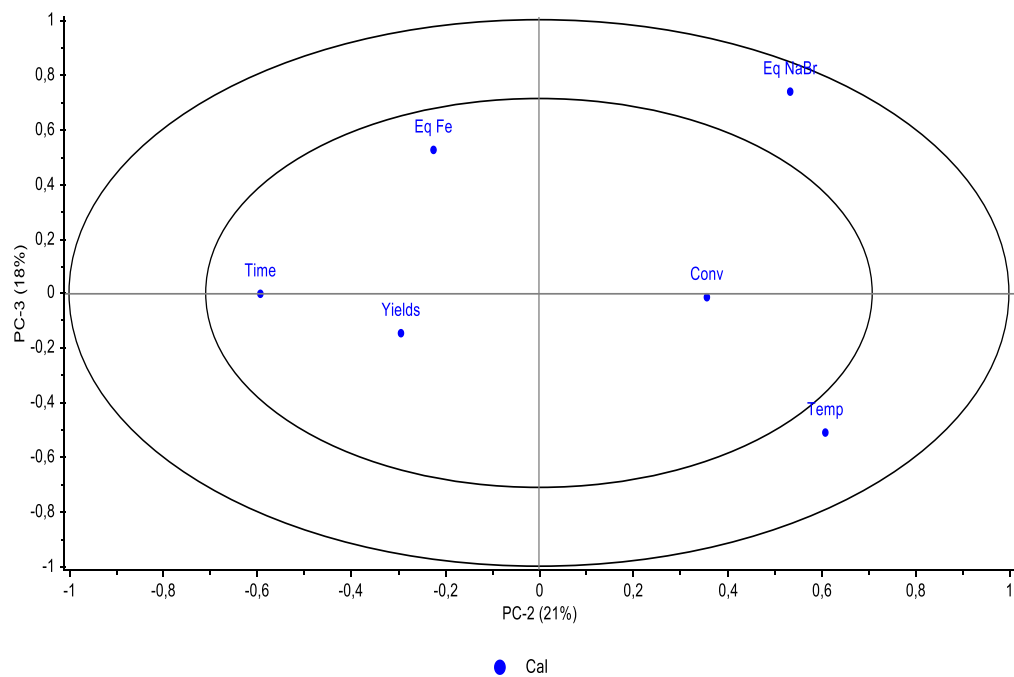


Figure 1S. PCA analysis of the scope

2. Spectroscopic analyses of FeCl₃•6H₂O

Raman analysis was performed on a Horiba Jobin-Yvon Labram 1B Confocal apparatus, Laser Ar/Kr from 100 mW to 647.1 nm; Simple Edge Filter: observation from 150 cm⁻¹; detector CCD30-11 1024x256 Pixels.

Mass analyses were performed on a Quattro-Micro mass spectrometer equipped with an Electrospray (ESI) probe (Waters Micromass, Wythenshawe, Manchester, UK). The triple quadrupole MS was operated in full scan mode (Range 0 to 500 Da) with compounds being ionised in the negative and/or positive electrospray ionisation mode. The detection conditions were: capillary potential 3.5 kV, cone potential 30 V, source temperature 120 °C, desolvation temperature 450 °C, cone gas flow 50 L/h, and desolvation gas flow 450 L/h. Nitrogen was the nebuliser gas.

Raman analyses

FeCl₃•6H₂O has been analysed by Raman spectroscopy to confirm its composition as melted salt. 1g of FeCl₃•6H₂O was put in a sealed tube and heated at 80°C for a few second. The salt instantly melted.

Mass spectrometry analyses

Melted FeCl₃•6H₂O and melted salts mixtures have been analysed by direct infusion mass spectrometry using anisole as solvent, and with different preparation mode. 1 or 2 equivalents of FeCl₃•6H₂O and, in the case of the melted salt mixture, 1 equivalent of the natural salt are put in a sealed tube under heating.

2.1 Characterisation of FeCl₃•6H₂O

2.1.1 Raman studies

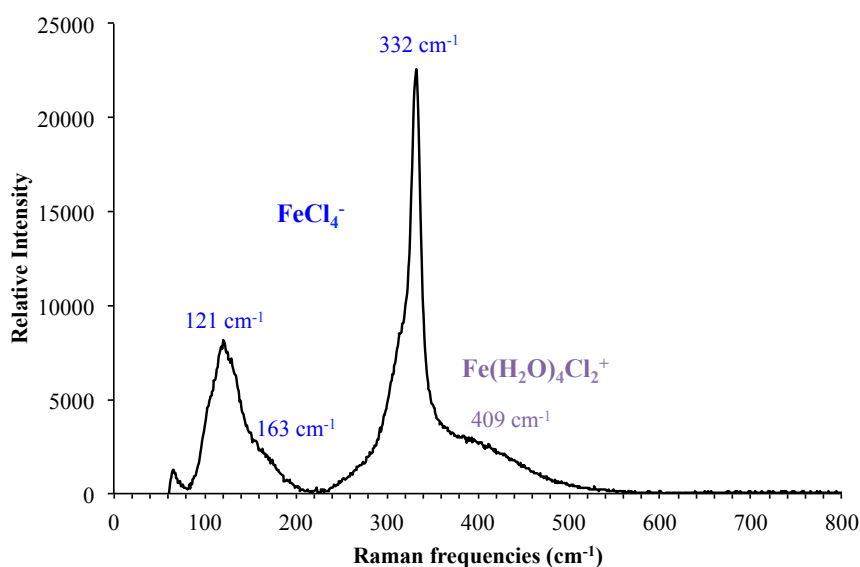


Figure 2S. Raman spectrum of melted FeCl₃.6H₂O.

Table 2S. Comparison of Raman frequencies of melted FeCl₃•6H₂O between data from literature and the present study

Raman frequencies of melted FeCl ₃ •6H ₂ O (cm ⁻¹)				
	FeCl ₄ ⁻			Fe(H ₂ O) ₄ Cl ₂ ⁺
Sharma et al.	115 m	154 vw	337 vs	425 m bd
In this paper	121 m	163 vw	332 vs	409 m bd

m: medium, vw: very weak, vs: very strong, bd: broad.

2.1.2 Direct injection mass spectrometry studies

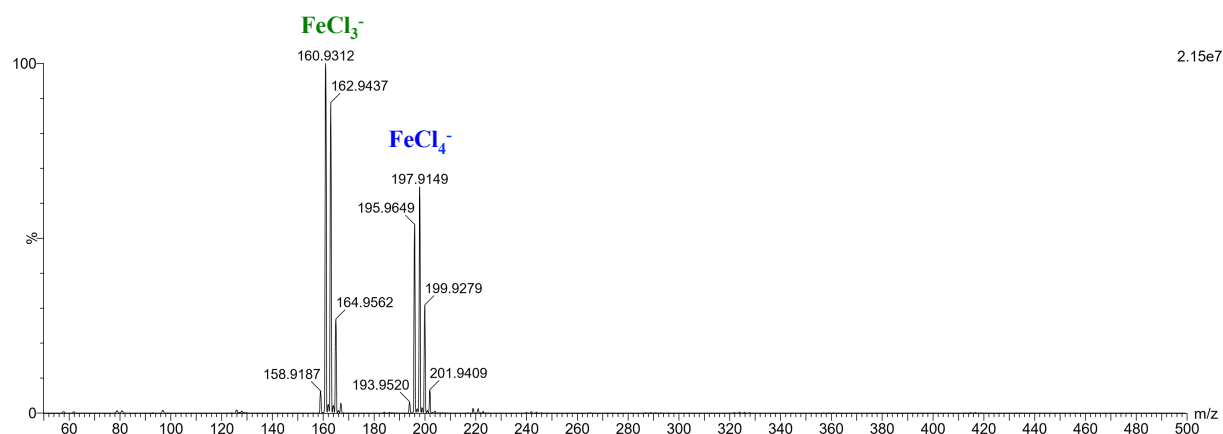


Figure 3S. Direct infusion electrospray ionization in negative mode of FeCl₃·6H₂O after heating at 80 °C.

2.2 Characterisation of FeCl₃·6H₂O in presence of NaBr

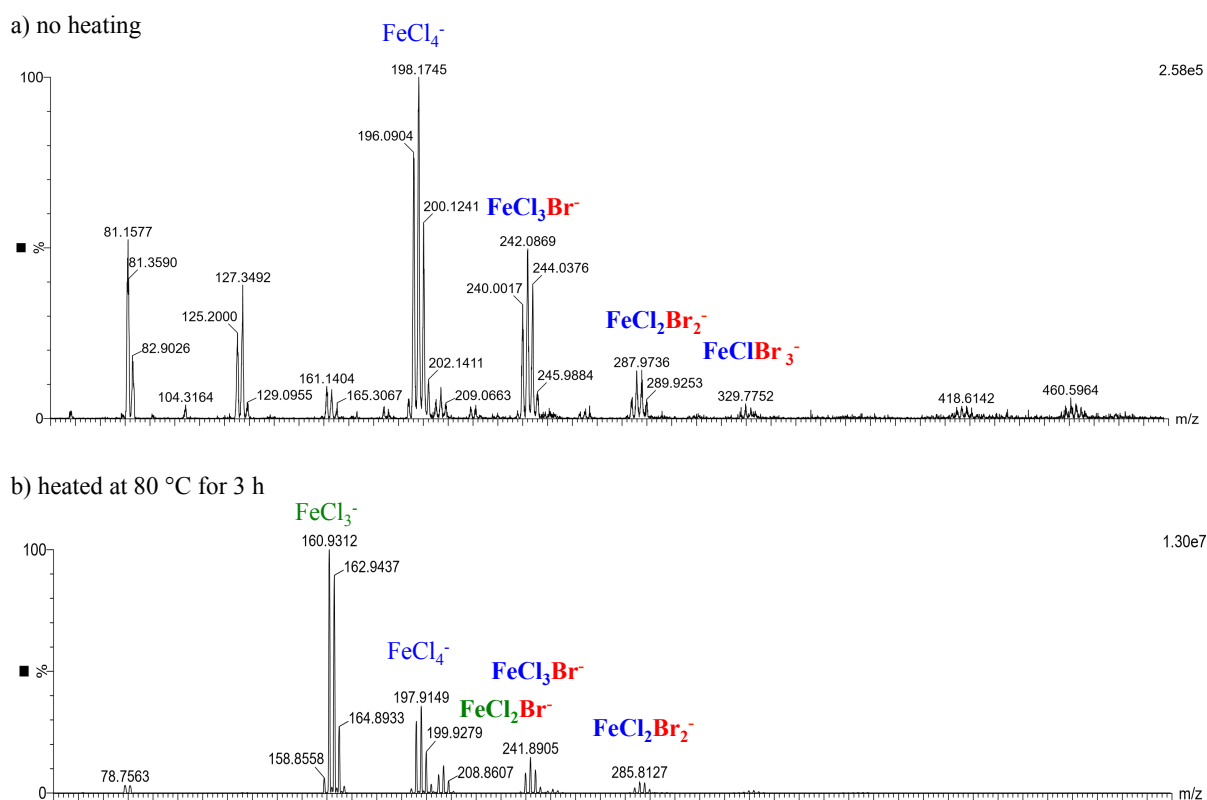


Figure 4S. Direct infusion electrospray ionization in negative mode of FeCl₃·6H₂O in presence of NaBr: a) not heated; b) heated at 80 °C for 3 hrs.

2.3 Characterisation of $\text{FeCl}_3 \cdot 6\text{H}_2\text{O}$ in presence of KNO_3

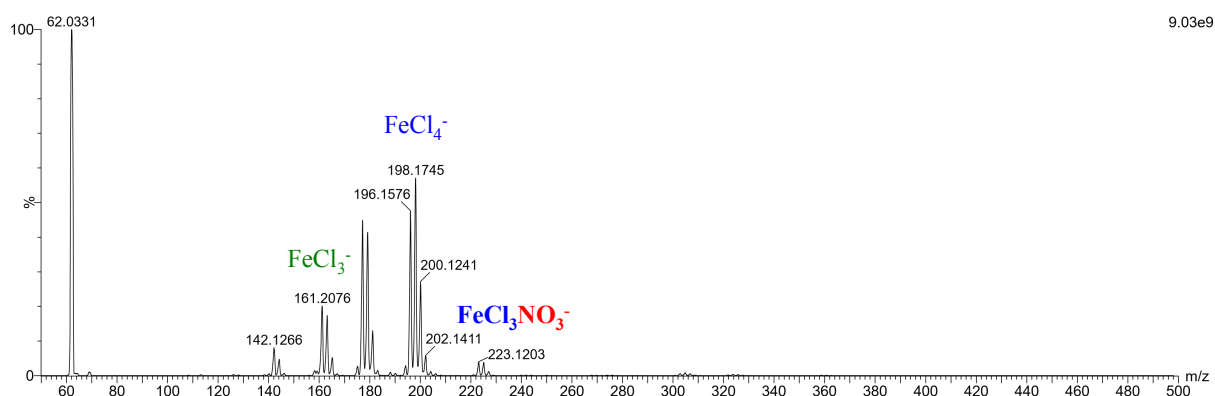


Figure 5S. Direct infusion electrospray ionization in negative mode of $\text{FeCl}_3 \cdot 6\text{H}_2\text{O}$ in presence of KNO_3 after heating at 80°C .

2.4 Characterisation of $\text{FeCl}_3 \cdot 6\text{H}_2\text{O}$ in presence of KSCN

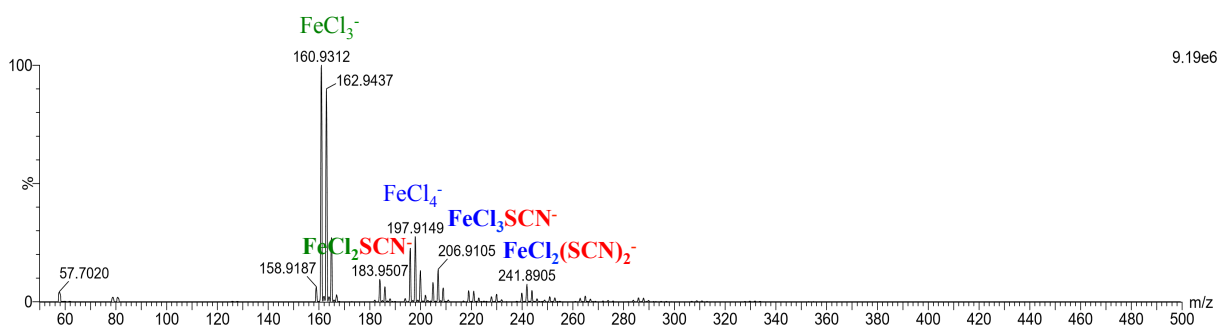


Figure 6S. Direct infusion electrospray ionization in negative mode of $\text{FeCl}_3 \cdot 6\text{H}_2\text{O}$ in presence of KSCN after heating at 80°C .

3. Computational calculations

3.1 Methods

Gas phase geometry optimisations and single point energy evaluations were performed using def2-SVP double- ζ basis set at the PBE1PBE level of theory, as implemented in Gaussian 16-A.03⁹. The Gibbs free energy of the optimised conformers was calculated at 298.15 K. Minimizations were performed with the Berny algorithm using GEDIIS in redundant internal coordinates. Tight linear equation convergence and quadratic convergence SCF method have been used. No constraints relative to the positive or negative charges on ions were applied. Gausview 6.0¹⁰ was used for visualization of orbitals. The SCF convergence default was used for Gaussian and the symmetry constraint was ignored. A hybrid functional, which include a mixture of Hartree-Fock exchange with DFT exchange-correlation, was used. The PBE1PBE functional that uses 25% exchange and 75% correlation weighting, is known in the literature as PBE0. The 1996 pure functional of Perdew, Burke and Ernzerhof was made into a hybrid by Adamo¹¹. The double- ζ basis set def2-SVP¹² with polarization functions was used. The D3 version of Grimme dispersion with Becke-Johnson damping was added for empirical dispersion¹³ (typically used for non-covalent interactions, supramolecular complexes in solution). The ElectroStatic Potential map (ESP) was generated at isovalue: 0.03. Partial charges are created due to the asymmetric distribution of electrons in chemical bonds; calculating them can afford an interesting picture of electron density distribution in the molecule and therefore of its properties such as reactivity. As there exist several ways to calculate atomic charges, we selected relevant atomic charge types. Mulliken and CM5¹⁴ are derived from population analysis of wavefunctions. Hirshfeld charges¹⁵ are obtained by partitioning of electron density distributions while APT (Atomic Polar Tensor) charges¹⁶ are derived from dipole-dependent properties. Since the dipole moment is sensitive to the level of calculation, so are the APT charges. Given the high level of basis sets used in our study, we can be confident in its reliability and the importance of dipolar interactions towards reactivity in this work led us to rely strongly on this model for various interpretations.

3.2 DFT calculations of the ion pair complexes

3.2.1 Procedure

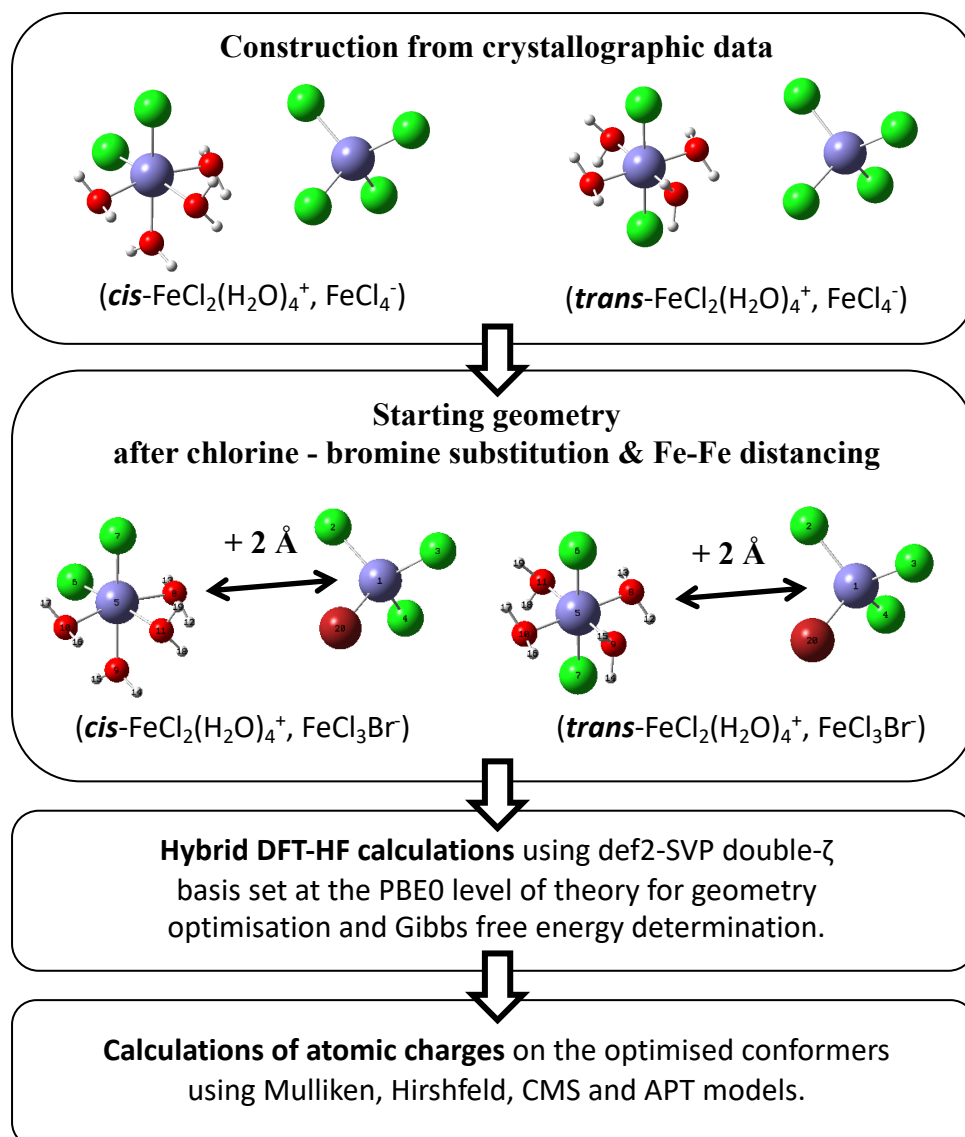


Figure 7S. Procedure for geometry optimisation of $(\text{trans-FeCl}_2(\text{H}_2\text{O})_4)^+$, FeCl_3Br^- and $(\text{cis-FeCl}_2(\text{H}_2\text{O})_4)^+$, FeCl_3Br^-

3.2.2 Choice of the system studied

Calculations were made with and without the hydrogen-bonded water molecule (see Scheme 1, main text). No significant change in bond distances and charges were noted (see below), so the simplified complex (without HB-water) was preferred for the rest of the calculations, mainly to remove uncertainty on the positioning of the extra water molecule. Regarding the gas phase vs hydrated system, supplementary calculations were run both using the implicit IEFPCM model (with water as solvent) and eight explicit water molecules (Table 3-5S). Applying an implicit IEFPCM solvation model did not

change drastically the geometry of the stable complex, nor the charge on the considered halogen atoms (Br20 and Cl6/Cl7); the calculations were therefore executed in the gas phase for computing-time considerations.

Table 3S. APT atomic charge on Br20 and Cl6/Cl7 atoms and distances in angstrom between Br20 and Cl6/Cl7 atoms

Conformations	Q_{Br20}	Q_{Cl6}	$d(\text{Br20-Cl6}) \text{ \AA}$
<i>cis</i> -FeCl ₂ (H ₂ O) ₄ ⁺ ,(FeCl ₃ Br) ⁻	0.246167	-0.419038	2.835
<i>cis</i> -FeCl ₂ (H ₂ O) ₄ ⁺ ,(FeCl ₃ Br) ⁻ 1H ₂ O - A	0.250893	-0.527982	2.876
<i>cis</i> -FeCl ₂ (H ₂ O) ₄ ⁺ ,(FeCl ₃ Br) ⁻ 1H ₂ O - B	0.205979	-0.386993	2.913
<i>cis</i> -FeCl ₂ (H ₂ O) ₄ ⁺ ,(FeCl ₃ Br) ⁻ 1H ₂ O - C	0.212742	-0.463271	2.866
<i>cis</i> -FeCl ₂ (H ₂ O) ₄ ⁺ ,(FeCl ₃ Br) ⁻ PCMwater	0.333764	-0.476349	2.790
Conformations	Q_{Br20}	Q_{Cl7}	$d(\text{Br20-Cl7}) \text{ \AA}$
<i>trans</i> -FeCl ₂ (H ₂ O) ₄ ⁺ ,(FeCl ₃ Br) ⁻	0.300333	-0.675900	2.876
<i>trans</i> -FeCl ₂ (H ₂ O) ₄ ⁺ ,(FeCl ₃ Br) ⁻ 1H ₂ O - A	0.274532	-0.715487	2.919
<i>trans</i> -FeCl ₂ (H ₂ O) ₄ ⁺ ,(FeCl ₃ Br) ⁻ 1H ₂ O - B	0.227341	-0.524004	2.945
<i>trans</i> -FeCl ₂ (H ₂ O) ₄ ⁺ ,(FeCl ₃ Br) ⁻ 1H ₂ O - C	0.221651	-0.592300	2.917
<i>trans</i> -FeCl ₂ (H ₂ O) ₄ ⁺ ,(FeCl ₃ Br) ⁻ PCMwater	0.517798	-0.834074	2.808

Table 4S. Iron chloride hexahydrate models (**geom022**, cis) without the hydrogen-bonded water molecule and with the water molecule placed in 3 arbitrary positions; energy and bond distances summarised in Table 3S.

geom	Starting geometry	Optimised geometry
022		
022-A		
022-B		
022-C		

Table 5S. Iron chloride hexahydrate models (**geom121**, trans) without the hydrogen-bonded water molecule and with the water molecule placed in 3 arbitrary positions; energy and bond distances summarised in Table 3S.

geom	Starting geometry	Optimised geometry
121		
121-A		
121-B		
121-C		

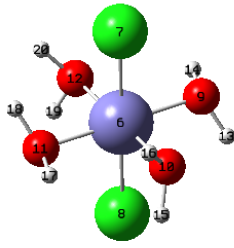
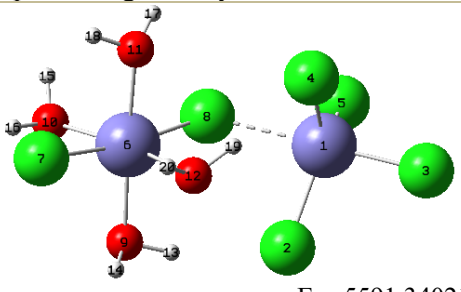
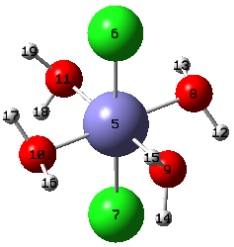
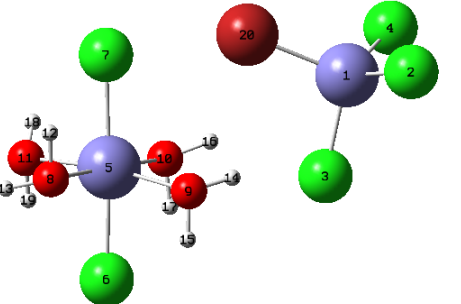
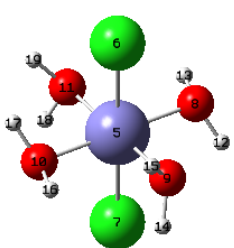
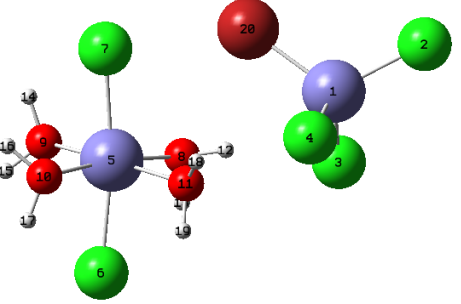
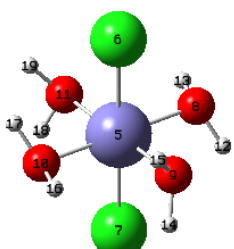
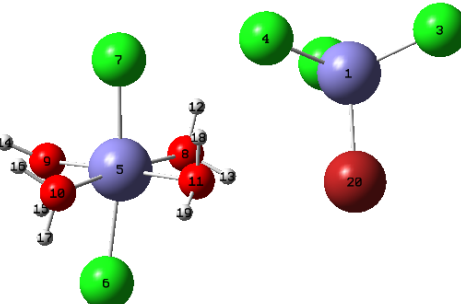
3.2.3 Results - Optimised geometry and Gibbs free energy

Table 6S. Iron chloride hexahydrate models (**geom02X**) generated from crystal structures where the starting geometries are brought apart ($d(\text{Fe}-\text{Fe}) = 8.0 \text{ \AA}$) compared to the crystalline state.

geom	Starting geometry	Optimised geometry
020 ^d		 E= -5591.455447 h.
021 ^d		 E= -7705.098971 h.
022 ^d		 E= -7705.105329 h.
023 ^d		 E= -7705.092754 h.

^d from geom01X, tearing apart of the ions : $d(\text{Fe}-\text{Fe})$ from 6.0 \AA to 8.0 \AA .

Table 7S. Iron chloride hexahydrate models (**geom12X**) generated from crystal structures where the cis configuration formed by the two chloride atoms of the hydrated cation in the crystalline state is converted into a trans configuration and where the ions are brought apart ($d_{\text{Fe-Fe}} = 8.0 \text{ \AA}$) compared to the crystalline state.

geom	Starting geometry	Optimised geometry
120 ^d		
121 ^d		
122 ^d		
123 ^d		

^d from **geom11X**, tearing apart of the ions : $d(\text{Fe-Fe})$ from 6.0 \AA to 8.0 \AA .

3.2.4 Results – Partial atomic charges of the optimised conformers

Table 8S. Atomic charges (derived from different models) for **geom 010** iron complex

<i>cis(FeCl₂)⁺(FeCl₄)⁻</i>				
geom010	Mulliken	Hirshfeld	CM5	APT
Fe1	0.352313	0.158794	0.416713	1.135420
Cl2	-0.210251	-0.109662	-0.175509	-0.320099
Cl3	-0.147286	-0.095226	-0.162548	-0.697471
Cl4	-0.182974	-0.101090	-0.167660	-0.318090
Cl5	-0.097654	-0.030241	-0.100043	0.175712
Fe6	0.449675	0.081294	0.380501	0.861703
Cl7	-0.289574	-0.193309	-0.239291	-0.377643
Cl8	-0.443992	-0.300342	-0.344873	-0.715666
O9	-0.259730	-0.178929	-0.569947	-0.337579
O10	-0.243999	-0.181564	-0.567575	-0.384041
O11	-0.209690	-0.161401	-0.548611	-0.616568
O12	-0.240981	-0.184017	-0.564161	-0.603554
H13	0.182673	0.137792	0.306352	0.149219
H14	0.198160	0.168210	0.335405	0.292771
H15	0.176317	0.127351	0.296744	0.186865
H16	0.191506	0.161269	0.330394	0.252816
H17	0.204225	0.192708	0.362604	0.305948
H18	0.198961	0.176440	0.343062	0.371525
H19	0.204566	0.190997	0.360578	0.260902
H20	0.167737	0.140931	0.307873	0.377830

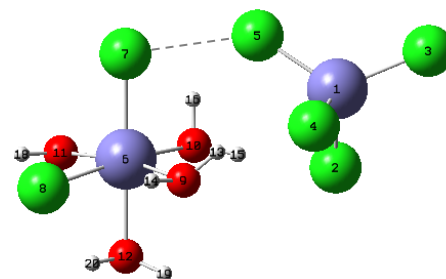


Table 9S. Atomic charges (derived from different models) for **geom022** iron complex

<i>cis(FeCl₂)⁺(FeCl₃Br)⁻</i>				
geom022	Mulliken	Hirshfeld	CM5	APT
Fe1	0.325365	0.131265	0.373346	1.125163
Cl2	-0.151788	-0.100017	-0.167846	-0.678430
Cl3	-0.215387	-0.117523	-0.183513	-0.338378
Cl4	-0.191821	-0.111345	-0.177980	-0.342531
Fe5	0.459064	0.075035	0.371562	0.846512
Cl6	-0.295095	-0.192171	-0.238100	-0.419038
Cl7	-0.447697	-0.303749	-0.348161	-0.706360
O8	-0.265976	-0.180178	-0.571209	-0.361690
O9	-0.247171	-0.181441	-0.567580	-0.405628
O10	-0.211883	-0.163186	-0.550088	-0.611340
O11	-0.240522	-0.184165	-0.564795	-0.604488
H12	0.182539	0.133903	0.302234	0.167977
H13	0.200135	0.169918	0.337195	0.296652
H14	0.178470	0.127044	0.295907	0.199994
H15	0.195358	0.164281	0.333048	0.258946
H16	0.204124	0.192022	0.362039	0.307208
H17	0.198163	0.175031	0.341640	0.371626
H18	0.204160	0.190230	0.360007	0.265962
H19	0.167200	0.140267	0.307223	0.381676
Br20	-0.047238	0.034763	-0.014947	0.246167

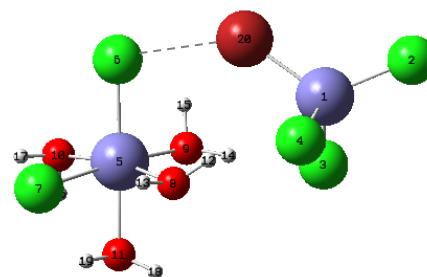
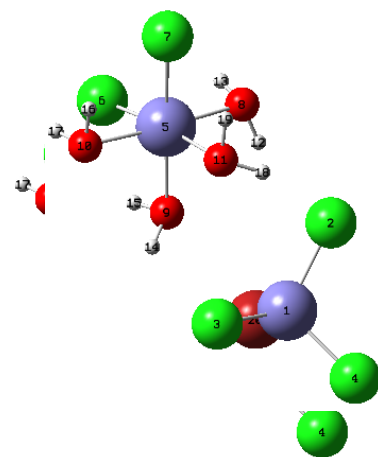


Table 10S. Atomic charges (derived from different models) for **geom021** iron complex

<i>cis</i> (FeCl ₂) ⁺ (FeCl ₃ Br) ⁻				
geom021	Mulliken	Hirshfeld	CM5	APT
Fe1	0.329039	0.153109	0.405527	1.322845
Cl2	-0.166149	-0.058317	-0.126895	-0.224306
Cl3	-0.140660	-0.060936	-0.128465	-0.210135
Cl4	-0.082092	-0.055416	-0.125942	-0.581034
Fe5	0.432466	0.084005	0.377608	1.236323
Cl6	-0.443536	-0.303025	-0.348346	-0.680546
Cl7	-0.418743	-0.296277	-0.342683	-0.817414
O8	-0.224343	-0.170486	-0.558589	-0.363236
O9	-0.256922	-0.176700	-0.566272	-0.265817
O10	-0.220199	-0.185356	-0.566698	-0.605679
O11	-0.238476	-0.183061	-0.566862	-0.341628
H12	0.186817	0.159204	0.330183	0.159487
H13	0.203860	0.178770	0.345416	0.308925
H14	0.201378	0.159381	0.329491	0.144287
H15	0.178132	0.152928	0.320147	0.198280
H16	0.181082	0.156349	0.322607	0.346698
H17	0.185387	0.162153	0.328687	0.340669
H18	0.182604	0.146228	0.316757	0.144028
H19	0.181314	0.153115	0.320029	0.226417
Br20	-0.070958	-0.015684	-0.065719	-0.338163

**Table 11S.** Atomic charges (derived from different models) for **geom023** iron complex

<i>cis</i> (FeCl ₂) ⁺ (FeCl ₃ Br) ⁻				
Geom023	Mulliken	Hirshfeld	CM5	APT
Fe1	0.322427	0.141351	0.387747	1.137586
Cl2	-0.085103	-0.022643	0.093701	0.148825
Cl3	-0.129751	-0.086897	0.155609	-0.667956
Cl4	-0.234758	-0.107749	0.173087	-0.299791
Fe5	0.462197	0.080806	0.377957	0.912715
Cl6	-0.432285	-0.303870	0.348692	-0.678882
Cl7	-0.345323	-0.227004	0.272039	-0.508613
O8	-0.243039	-0.177760	0.572605	-0.276293
O9	-0.228182	-0.183954	0.562407	-0.575442
O10	-0.205094	-0.159414	0.548058	-0.611628
O11	-0.252869	-0.186202	0.572228	-0.416030
H12	0.177582	0.144986	0.315228	0.166127
H13	0.184955	0.161380	0.328789	0.270000
H14	0.176156	0.183093	0.351593	0.233627
H15	0.177016	0.141568	0.307325	0.393920
H16	0.200860	0.188291	0.359128	0.307107
H17	0.198860	0.180061	0.347114	0.381103
H18	0.178775	0.135100	0.304856	0.203093
H19	0.175671	0.138012	0.307844	0.226280
Br20	-0.098094	-0.039164	0.089166	-0.345748

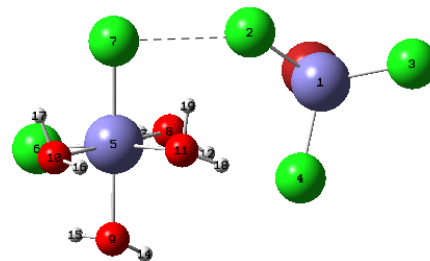
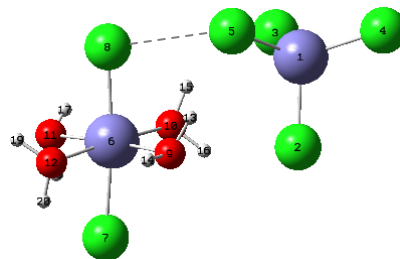


Table 12S. Atomic charges (derived from different models) for **geom110** iron complex

trans(FeCl₂)⁺(FeCl₄)⁻

Geom110	Mulliken	Hirshfeld	CM5	APT
Fe1	0.337988	0.162559	0.424305	1.126466
Cl2	-0.167314	-0.092088	-0.158340	-0.245963
Cl3	-0.163022	-0.096676	-0.163407	-0.279110
Cl4	-0.138475	-0.087148	-0.154592	-0.714202
Cl5	-0.115271	-0.035298	-0.105938	0.071612
Fe6	0.452709	0.082651	0.383216	0.899851
Cl7	-0.448245	-0.313064	-0.355877	-0.740514
Cl8	-0.370799	-0.263008	-0.307364	-0.406520
O9	-0.219956	-0.168214	-0.558042	-0.324400
O10	-0.252198	-0.172765	-0.565418	-0.283790
O11	-0.229957	-0.179817	-0.563129	-0.629365
O12	-0.234853	-0.169531	-0.556062	-0.651880
H13	0.179215	0.135872	0.305752	0.165440
H14	0.205550	0.190583	0.360830	0.298570
H15	0.181095	0.143616	0.312742	0.150583
H16	0.201887	0.164702	0.333298	0.206531
H17	0.205510	0.192089	0.360904	0.277461
H18	0.179715	0.150409	0.317444	0.368067
H19	0.212541	0.197186	0.364937	0.333913
H20	0.183879	0.157942	0.324743	0.377250

**Table 13S.** Atomic charges (derived from different models) for **geom114** iron complex

trans(FeCl₂)⁺(FeCl₃Br)⁻

Geom114	Mulliken	Hirshfeld	CM5	APT
Fe1	0.321667	0.132941	0.378438	1.164408
Cl2	-0.194473	-0.109965	-0.176832	-0.349724
Cl3	-0.140915	-0.092057	-0.160598	-0.662486
Cl4	-0.194992	-0.109876	-0.176621	-0.345130
Cl5	-0.466275	-0.314982	-0.357800	-0.658997
Cl6	-0.350084	-0.221624	-0.265456	-0.540955
Fe7	0.475295	0.073515	0.369538	0.856117
O8	-0.262678	-0.182301	-0.571394	-0.387549
H9	0.184006	0.133195	0.301720	0.179693
O10	-0.206153	-0.164201	-0.550430	-0.575153
H11	0.193279	0.171441	0.339033	0.360926
O12	-0.208712	-0.164419	-0.551007	-0.604901
H13	0.205244	0.190492	0.360020	0.295459
O14	-0.258791	-0.185620	-0.573809	-0.408089
H15	0.173088	0.152119	0.319945	0.290243
H16	0.192133	0.169841	0.337260	0.368936
H17	0.200639	0.188252	0.358428	0.305052
H18	0.185958	0.160882	0.328729	0.287055
H19	0.183972	0.134587	0.303025	0.185186
Br20	-0.032211	0.037772	-0.012199	0.239909

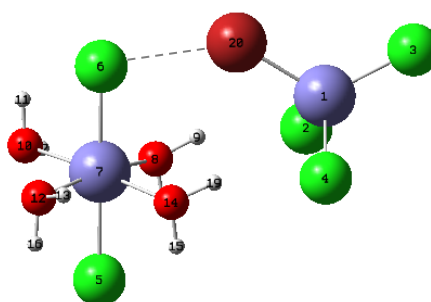
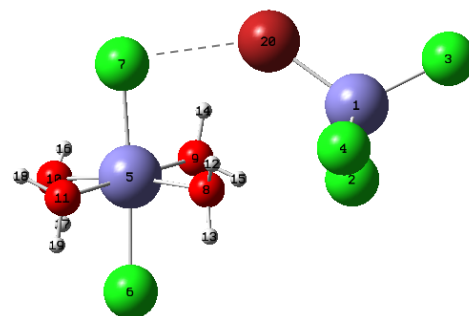


Table 14S. Atomic charges (derived from different models) for **Geom111** iron complex***trans*(FeCl₂)⁺(FeCl₃Br)⁻**

Geom111	Mulliken	Hirshfeld	CM5	APT
Fe1	0.332668	0.139694	0.390041	1.194299
Cl2	-0.182698	-0.097859	-0.164648	-0.326106
Cl3	-0.132727	-0.087346	-0.156187	-0.645792
Cl4	-0.172159	-0.109454	-0.176069	-0.380575
Fe5	0.463647	0.062476	0.359414	0.881501
Cl6	-0.474012	-0.325864	-0.368191	-0.699593
Cl7	-0.389802	-0.268903	-0.311709	-0.556371
O8	-0.241732	-0.162352	-0.560323	-0.299227
O9	-0.242200	-0.181896	-0.569230	-0.391238
O10	-0.234449	-0.173917	-0.560219	-0.639360
O11	-0.223959	-0.175705	-0.560204	-0.600065
H12	0.203603	0.175426	0.344136	0.202253
H13	0.197134	0.181265	0.349573	0.265636
H14	0.182275	0.144835	0.314000	0.229655
H15	0.194523	0.146718	0.316143	0.219123
H16	0.206244	0.194105	0.362472	0.310165
H17	0.191781	0.163587	0.330714	0.370123
H18	0.206873	0.192890	0.361158	0.323467
H19	0.175512	0.154738	0.322051	0.348859
Br20	-0.060521	0.027531	-0.022954	0.193248



3.3 DFT calculations of the ion pair complexes in presence of anisole

3.3.1 Procedure

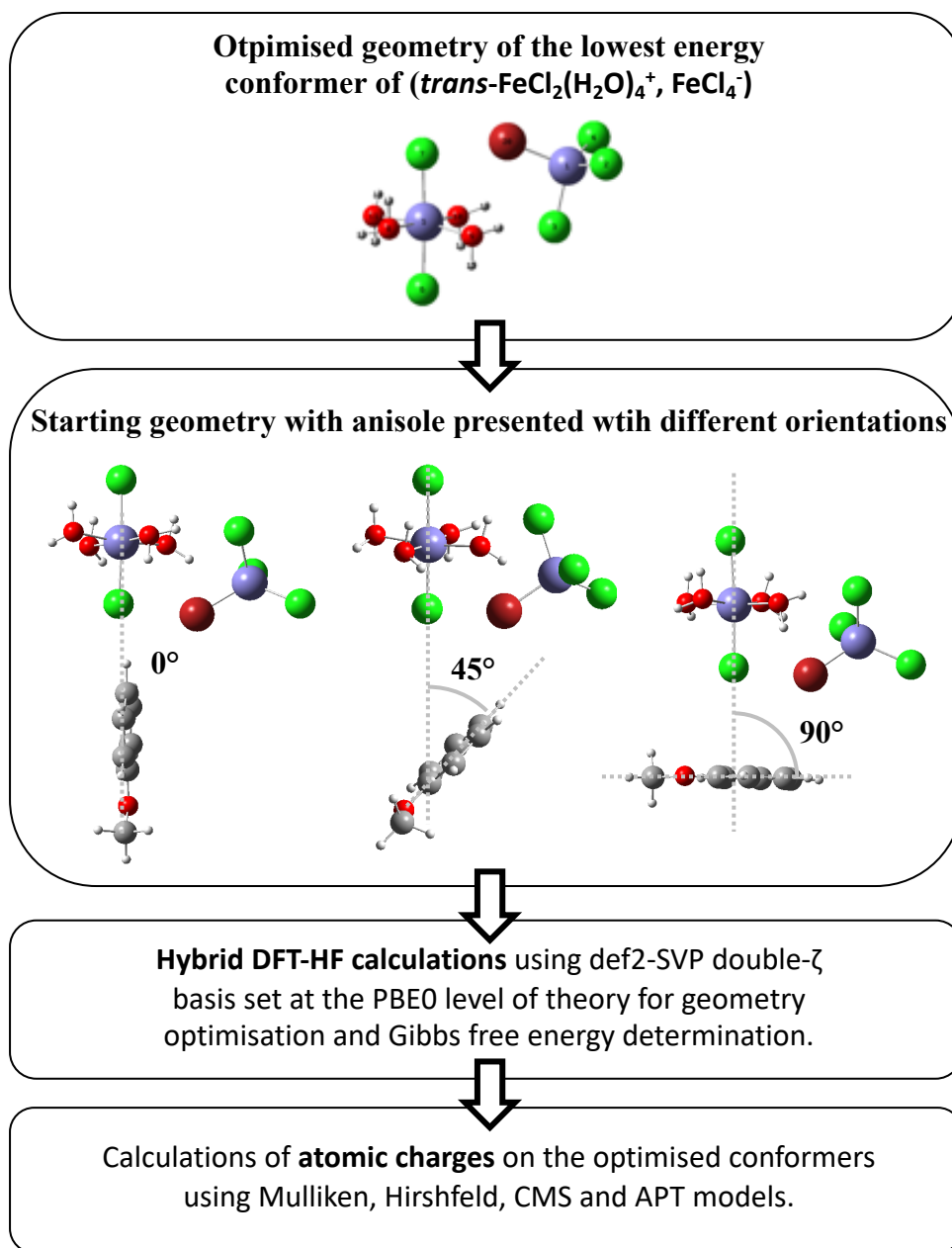


Figure 8S. Procedure for geometry optimisation of (*trans*-FeCl₂(H₂O)₄⁺, FeCl₃Br⁻) and (*cis*-FeCl₂(H₂O)₄⁺, FeCl₃Br⁻) in presence of anisole.

3.3.2 Results - Optimised geometry and Gibbs free energy

Table 15S. Initial and optimised geometries of iron chloride hexahydrate models (**geom211-213**) generated from optimised iron salt trans configuration models to which an anisole molecule was added in different orientations.

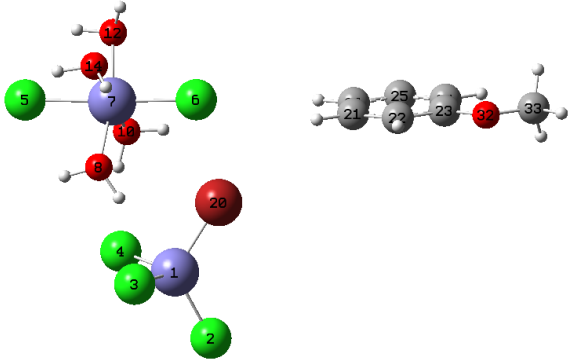
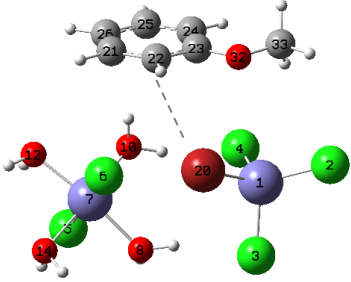
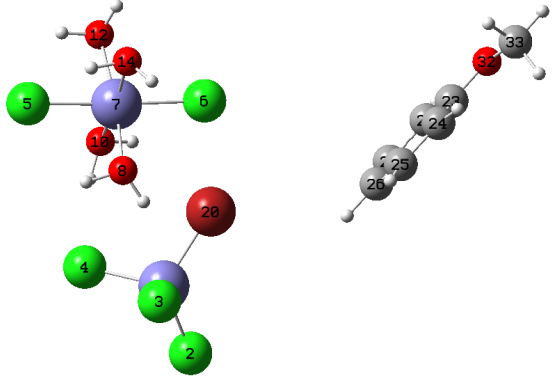
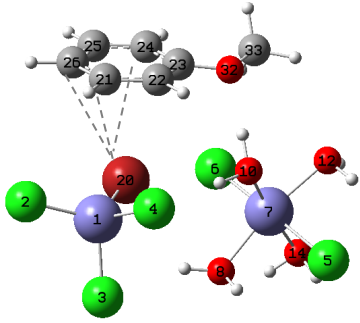
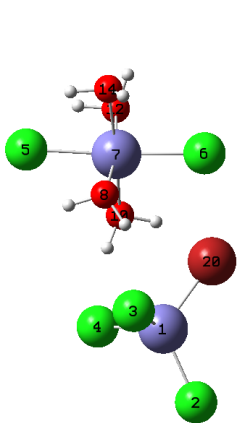
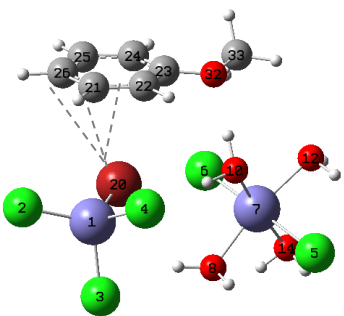
geom	Starting geometry	Optimised geometry
211		
212		
213		

Table 16S. Characteristic distances (in Å) between selected atoms in complexes **geom211-213**.

	211		212		213	
	Distance (Å)		Bond distance (Å)		Bond distance (Å)	
	Start	End	Start	End	Start	End
Cl(6)-Br(20)	2.89	2.81	2.86	2.84	2.86	2.84
C(22)-Br(20)	5.34	3.48	6.17	3.59	5.26	3.59
C(24)-Br(20)	9.51	3.63	6.14	3.52	4.90	3.51
C(25)- Br(20)	5.79	5.47	4.94	3.61	4.17	3.61
C(26)-Br(20)	4.54	5.32	4.25	3.68	4.00	3.68

Table 17S. Energies for the complex between the iron adduct and anisole (**geom211-213**)

geom	E /hartree	ZPE /hartree	ΔE /kcal.mol ⁻¹
211	-8051.263407	0.249209	+3.7
212	-8051.269328	0.249997	0.0
213	-8051.269341	0.250026	0.0

3.3.3 Results – Partial atomic charges of the optimised conformers

Table 18S. Atomic charges (derived from different models) for **geom211** complex

		Mulliken	Hirshfeld	CM5	APT
Fe	1	0.327368	0.128363	0.371937	1.128163
Cl	2	-0.165641	-0.106910	-0.174225	-0.675599
Cl	3	-0.196671	-0.121250	-0.187377	-0.382860
Cl	4	-0.196964	-0.095416	-0.162671	-0.333783
Cl	5	-0.464239	-0.314619	-0.356803	-0.702586
Cl	6	-0.331956	-0.210415	-0.253882	-0.503195
Fe	7	0.480428	0.073848	0.371400	0.885466
O	8	-0.261737	-0.181471	-0.570492	-0.381979
H	9	0.184570	0.133901	0.302385	0.182449
O	10	-0.251964	-0.182120	-0.575177	-0.407982
H	11	0.224718	0.133002	0.306436	0.317572
O	12	-0.216471	-0.164140	-0.550053	-0.582279
H	13	0.204711	0.192508	0.361226	0.318240
O	14	-0.234406	-0.181028	-0.565009	-0.635539
H	15	0.173098	0.149484	0.316974	0.367117
H	16	0.192986	0.167018	0.334273	0.343243
H	17	0.175540	0.128629	0.299248	0.171145
H	18	0.191483	0.167127	0.335027	0.281008
H	19	0.210360	0.190867	0.359611	0.298418

Br	20	-0.025420	0.059462	0.010200	0.284122
C	21	-0.066386	-0.033040	-0.090350	-0.014206
C	22	-0.069974	-0.056896	-0.108444	-0.185595
C	23	0.201713	0.074570	0.090656	0.457615
C	24	-0.100848	-0.066003	-0.117628	-0.141707
C	25	-0.013160	-0.036233	-0.091179	0.045698
C	26	-0.023752	-0.049673	-0.105666	-0.122872
H	27	0.033157	0.046687	0.102465	0.074858
H	28	0.030288	0.040526	0.100105	0.079375
H	29	0.017701	0.041001	0.099595	0.073169
H	30	0.028452	0.045879	0.100707	0.042552
H	31	0.023708	0.043594	0.098629	0.053544
O	32	-0.335265	-0.125151	-0.219556	-0.756645
C	33	0.098126	-0.000135	-0.118870	0.401220
H	34	0.045877	0.036241	0.094531	-0.022498
H	35	0.062981	0.044796	0.105089	0.038135
H	36	0.047585	0.026951	0.086843	0.006214

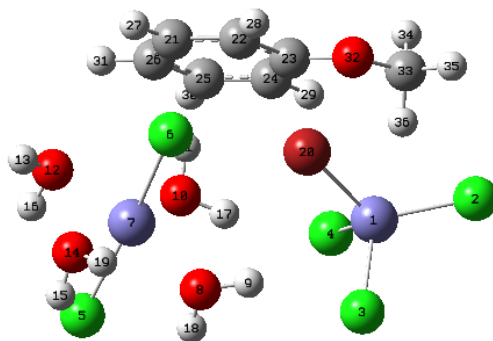


Table 19S. Atomic charges (derived from different models) for **geom212** complex

		Mulliken	Hirshfeld	CM5	APT
Fe	1	0.312157	0.126085	0.371733	1.144839
Cl	2	-0.157524	-0.105108	-0.172692	-0.656977
Cl	3	-0.185212	-0.121162	-0.187316	-0.400946
Cl	4	-0.195031	-0.102027	-0.168920	-0.335422
Cl	5	-0.465473	-0.315927	-0.357961	-0.712356
Cl	6	-0.348204	-0.218960	-0.262191	-0.545850
Fe	7	0.482219	0.070040	0.366858	0.887104
O	8	-0.260183	-0.178073	-0.568539	-0.378234
H	9	0.184609	0.137271	0.305928	0.186463
O	10	-0.279753	-0.192334	-0.582739	-0.470981
H	11	0.226896	0.126949	0.315373	0.424447
O	12	-0.219452	-0.162836	-0.548853	-0.608265
H	13	0.204335	0.191434	0.360322	0.319052
O	14	-0.236041	-0.182521	-0.566815	-0.631490
H	15	0.172930	0.148077	0.315598	0.367949
H	16	0.192149	0.164083	0.331122	0.359960
H	17	0.174793	0.125750	0.297231	0.187505
H	18	0.195909	0.171897	0.339793	0.281052
H	19	0.210569	0.190004	0.358802	0.295239
Br	20	-0.013830	0.058923	0.009250	0.311230
C	21	-0.028798	-0.034935	-0.090149	-0.016736
C	22	-0.061756	-0.061269	-0.111903	-0.158075
C	23	0.211414	0.071262	0.085396	0.413311
C	24	-0.080950	-0.062978	-0.114576	-0.150385
C	25	-0.019420	-0.037563	-0.092262	0.036231
C	26	-0.011256	-0.049443	-0.104493	-0.112832
H	27	0.032151	0.045840	0.101212	0.067150
H	28	0.019818	0.042834	0.102504	0.068923
H	29	0.017584	0.043346	0.101854	0.074558
H	30	0.027664	0.045361	0.100168	0.042632
H	31	0.025429	0.044095	0.098969	0.058929
O	32	-0.404047	-0.094442	-0.210107	-0.790148
C	33	0.103703	0.003028	-0.117087	0.384910
H	34	0.051689	0.039136	0.097743	-0.017839
H	35	0.063032	0.046280	0.107944	0.038195
H	36	0.057877	0.027895	0.088815	0.036857

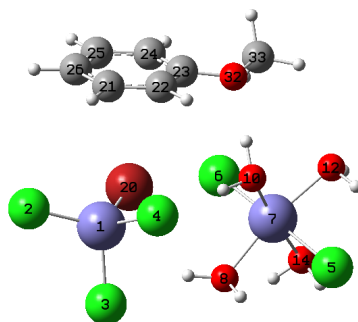
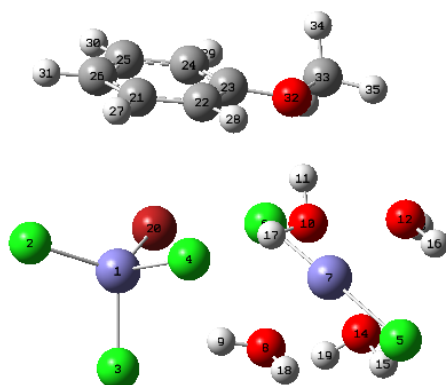


Table 20S. Atomic charges (derived from different models) for **geom213** complex

		Mulliken	Hirshfeld	CM5	APT
Fe	1	0.312208	0.126094	0.371740	1.144725
Cl	2	-0.157512	-0.105121	-0.172709	-0.656971
Cl	3	-0.185338	-0.121102	-0.187257	-0.400681
Cl	4	-0.194815	-0.101830	-0.168738	-0.335308
Cl	5	-0.465399	-0.315844	-0.357872	-0.712526
Cl	6	-0.348235	-0.219101	-0.262321	-0.546219
Fe	7	0.482313	0.070045	0.366837	0.886928
O	8	-0.260144	-0.178057	-0.568531	-0.378276
H	9	0.184588	0.137278	0.305920	0.186500
O	10	-0.279611	-0.192328	-0.582694	-0.470529
H	11	0.226830	0.127013	0.315411	0.424301
O	12	-0.219482	-0.162825	-0.548865	-0.608401
H	13	0.204324	0.191354	0.360265	0.319099
O	14	-0.236195	-0.182518	-0.566827	-0.631591
H	15	0.172911	0.148032	0.315550	0.368029
H	16	0.192064	0.164000	0.331039	0.360122
H	17	0.174659	0.125594	0.297105	0.186987
H	18	0.195971	0.171963	0.339858	0.281156
H	19	0.210581	0.190058	0.358839	0.295241
Br	20	-0.013729	0.058980	0.009309	0.311625
C	21	-0.028818	-0.034943	-0.090154	-0.016742
C	22	-0.061627	-0.061267	-0.111900	-0.158082
C	23	0.211330	0.071288	0.085422	0.413366
C	24	-0.080987	-0.062973	-0.114572	-0.150430
C	25	-0.019435	-0.037580	-0.092280	0.036181
C	26	-0.011279	-0.049452	-0.104502	-0.112831
H	27	0.032152	0.045846	0.101215	0.067134
H	28	0.019856	0.042823	0.102491	0.068987
H	29	0.017602	0.043338	0.101850	0.074542
H	30	0.027663	0.045359	0.100166	0.042639
H	31	0.025434	0.044103	0.098975	0.058853
O	32	-0.404051	-0.094470	-0.210125	-0.789988
C	33	0.103623	0.002992	-0.117130	0.384538
H	34	0.051721	0.039136	0.097746	-0.017802
H	35	0.063051	0.046232	0.107913	0.038218
H	36	0.057775	0.027838	0.088779	0.037207



References

- 1 E. Zysman-Colman, K. Arias and J. S. Siegel, *Can. J. Chem.*, 2009, **87**, 440–447.
- 2 L. J. Gooßen, C. Linder, N. Rodríguez, P. P. Lange and A. Fromm, *Chem. Commun.*, 2009, 7173.
- 3 M. Li and G. A. O'Doherty, *Org. Lett.*, 2006, **8**, 3987–3990.
- 4 P. J. Zeegers and M. J. Thompson, *Magn. Reson. Chem.*, 1992, **30**, 497–499.
- 5 C. P. Butts, L. Ebersson, M. P. Hartshorn and W. T. Robinson, *Acta Chem. Scand.*, 1996, **50**, 122–131.
- 6 R. Sathunuru, U. N. Rao and E. Biehl, *Arkivoc*, 2004, **2003**, 124.
- 7 H. M. Meshram, P. R. Goud, B. C. Reddy and D. A. Kumar, *Synth. Commun.*, 2010, **40**, 2122–2129.
- 8 D. Bhalerao and K. Akamanchi, *Synlett*, 2007, **2007**, 2952–2956.
- 9 M. J. Frisch, G. W. Trucks, H. B. Schlegel, G. E. Scuseria, M. A. Robb, J. R. Cheeseman, G. Scalmani, V. Barone, G. A. Petersson, H. Nakatsuji, X. Li, M. Caricato, A. V. Marenich, J. Bloino, B. G. Janesko, R. Gomperts, B. Mennucci, H. P. Hratchian, J. V. Ortiz, A. F. Izmaylov, J. L. Sonnenberg, D. Williams-Young, F. Ding, F. Lipparini, F. Egidi, J. Goings, B. Peng, A. Petrone, T. Henderson, D. Ranasinghe, V. G. Zakrzewski, J. Gao, N. Rega, G. Zheng, W. Liang, M. Hada, M. Ehara, K. Toyota, R. Fukuda, J. Hasegawa, M. Ishida, T. Nakajima, Y. Honda, O. Kitao, H. Nakai, T. Vreven, K. Throssell, J. A. Montgomery Jr., J. E. Peralta, F. Ogliaro, M. J. Bearpark, J. J. Heyd, E. N. Brothers, K. N. Kudin, V. N. Staroverov, T. A. Keith, R. Kobayashi, J. Normand, K. Raghavachari, A. P. Rendell, J. C. Burant, S. S. Iyengar, J. Tomasi, M. Cossi, J. M. Millam, M. Klene, C. Adamo, R. Cammi, J. W. Ochterski, R. L. Martin, K. Morokuma, O. Farkas, J. B. Foresman and D. J. Fox, *Gaussian16 Revision A.03*, 2016.
- 10 R. Dennington, T. A. Keith and J. M. Millam, *GaussView Version 6*, 2016.
- 11 C. Adamo, G. E. Scuseria and V. Barone, *J. Chem. Phys.*, 1999, **111**, 2889–2899.
- 12 F. Weigend and R. Ahlrichs, *Phys. Chem. Chem. Phys.*, 2005, **7**, 3297–3305.
- 13 S. Grimme, S. Ehrlich and L. Goerigk, *J. Comput. Chem.*, 2011, **32**, 1456–1465.
- 14 T. A. Manz and D. S. Sholl, *J. Chem. Theory Comput.*, 2012, **8**, 2844–2867.
- 15 F. L. Hirshfeld, *Theor. Chim. Acta*, 1977, **44**, 129–138.
- 16 J. Cioslowski, *J. Am. Chem. Soc.*, 1989, **111**, 8333–8336.